BIOFOULING METHODS

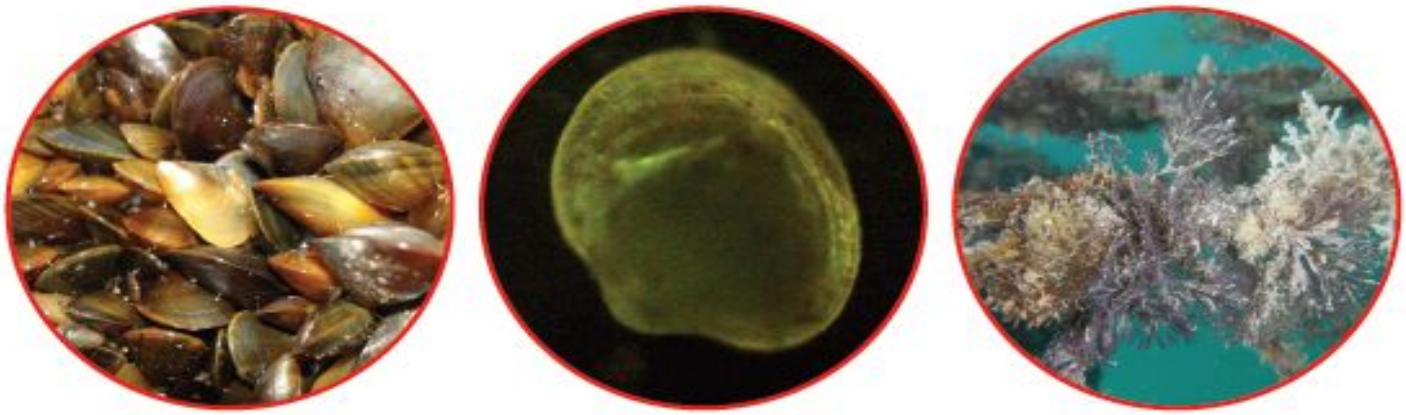

Editors

Sergey Dobretsov | David N. Williams | Jeremy C. Thomason

WILEY Blackwell

CONTENTS

List of Tables

ProbeBase (http://www.microbial-ecology.net/default.asp) [19, 20].

Table 1.3 Materials and equipment needed for the DAPI-based determination of bacterial abundance in biofilms.

Table 1.4 Materials and equipment needed for CARD-FISH.

Table 1.5 Hybridization solutions for horseradish labeled probes. Amount of compounds is enough for one probe hybridization. These solutions are stable for 2 months at –20 °C. Pre-warm the mixtures in water bath (60 °C) until dextran sulfate dissolves.

Table 1.6 Washing buffer solutions for horseradish labeled probes. Amount of compounds is enough to prepare 50 ml of washing solution. Pre-warm washing buffer at 37 °C in order to dissolve compounds.

Table 1.7 Amplification buffer solution. Can be used for any formamide concentration. p-iodophenylboronic acid (IPBA; 20 mg IPBA per 1 mg tyramide) enhances the CARD-FISH signal of tyramides labeled with Alexa488 and Alexa546 but does not work for tyramides labeled with Alexa350 and Cy3.

Table 1.8 Solutions for fixing and fluorescence *in situ* hybridization of biofilm samples for LSCM (see Notes 3–5).

Table 1.9 Hybridization buffer and wash buffer recipes for hybridization buffer containing 35% formamide.

Table 1.10 Concentrations of NaCl in washing buffer (48°C) at different concentrations of formamide in hybridization buffer (46°C).

List of Illustrations

English Channel: (a) common cyanobacteria, *Synechococcus* spp, on a scatter plot of SSC versus orange fluorescence (cyanobacteria distinguished from other phytoplankton by high orange fluorescence due to phycoerythrin); (b) pico and nanophytoplankton on a plot of SSC versus red fluorescence (chlorophyll *a*) with *Synechococcus* spp. gated out.

Figure 3.2 Flow cytometry data file of negative live control phytoplankton sample analyzed in WinMDI 2.9 software (Joseph Trotter, http://facs.scripps.edu); (a) orange versus red fluorescence properties of the phytoplankton, with region R1 (*Synechococcus*, cryptophyte, algae and debris); (b) SSC versus red fluorescence properties of the phytoplankton, with R1 gated out; (c) SSC versus green fluorescence properties of the phytoplankton stained with SYTOX Green, with R1 gated out and R2 representing nanoeukaryotes.

Figure 3.3 Flow cytometry data file of positive heat killed control and biocide-treated phytoplankton sample. Data analysed in WinMDI 2.8 software (Joseph Trotter, http://facs.scripps.edu): (a) orange versus red fluorescence properties of the phytoplankton, with region R1 (*Synechococcus*, cryptophyte algae and debris); (b) SSC versus red fluorescence properties of the phytoplankton, with R1 gated out; (c) SSC versus green fluorescence properties of the phytoplankton stained with SYTOX Green, with R1 gated out and R2 and R3 representing live and dead nanoeukaryotes respectively; (d) a biocide-treated sample, also with R1 gated out (NOTE: biocide treatment has altered SSC values and R3 has been positioned to account for this).

barcoded 16S primers, the samples are amplified, mixed, and sequenced on a 454 pyrosequencer. Subsequent assignment to samples based on barcodes, trimming of barcodes, and primer and low-quality read removal give rise to a set of unique sequences that will be used in all downstream analyses. Here, two possible analysis paths are shown. The first is taxon based, and all sequences are clustered into operational taxonomic units (OTUs) with a specific cutoff (here: 3%). These data can be used to calculate metrics for the alpha and beta diversity. The phylogenetic identity of the OTUs can be determined by searching a representative sequence in a 16S database. The second analysis is phylogeny-based. Here, the first step is the calculation of a phylogenetic tree from all sequences. This tree is the basis for estimation of beta diversity measures. Alpha diversity is estimated in combination with the taxonomic assignment of the single reads.

Figure 4.2 Example chromatogram. Each peak represents a base position and each “color” (depicted as gray levels) represents a base. The height of the peaks shows the light intensity as the florescent marked fragment passes the detector.

Figure 4.3 An overview of the different steps involved in microbial community analysis by DGGE, T-RFLP and ARISA techniques. Nucleic acids from an environmental sample are extracted, PCR amplified and the obtained bands are then analyzed. Note that the used primers amplify 16S rRNA in the case of DGGE and T-RFLP but its region in the case of ARISA.

Figure 4.4 Workflow indicating differences between BAC and Fosmid Clone libraries. This figure helps

determine what type of clone should be used, as well as special instructions for construction.

Chapter 05

Figure 5.1 Example of biofilm staining using different fluorescent markers. (A) *Staphylococcus aureus* ATCC 27217 biofilm stained with Syto9 and propidium iodide (Invitrogen). Green correspond to total cells and red/yellow correspond to membrane altered cells and also extracellular nucleic acids. (B) *Staphylococcus aureus* biofilm stained using Syto9 (total cells in green) and two lectins: ConA (red) and WGA (blue) (Invitrogen). (C) Amyloid fiber TasA stained with Thioflavine in *Bacillus subtilis* biofilms. (D) *Bacillus subtilis* 24-h biofilm of strain 168 carrying a GFP-*hag* transcriptional fusion and stained using the lipohilic marker FM4-64, which dye the cytoplasmic membrane in red (Invitrogen).

Figure 5.2 (a) Quantification of Chemchrome V6 fluorescence intensity loss (membrane permeabilization) during benzalkonium chloride C14 treatment (0.5% w/v) at five different depths in a *S. aureus* ATCC 6538 biofilm. (b) Representation of fluorescence loss in the biofilm during the biocide treatment after 0, 30 s, 1 min, 1 min 30 s, and 2 min of application. Each image corresponds to the 3D reconstruction of fluorescence in biofilm using the IMARIS software (Bitplane®).

Figure 5.3 Pathways leading to GacS/GacA-mediated gene expression. In all γ-proteobacteria GacS/GacA orthologs control “housekeeping” genes and horizontally acquired virulence genes regulating behaviors such as stress responses, attachment, motility, biofilm formation, virulence, and quorum sensing behaviors through the csr post-

transcriptional regulatory system. GacS, a transmembrane sensor kinase, perceives an environmental signal (likely acetate [30]) and autophosphorylates. Phosphorylated GacS then transphosphorylates a response regulator GacA, which binds to the promoter region upstream of the *csrB* sRNA gene to regulate its expression. The *csrB* regulatory RNA can sequester up to 18 CsrA molecules. Free CsrA protein binds to mRNA of target genes to either stabilize or de-stabilize messages. Stabilized messages are translated (*flhDC*) and de-stabilized messages are targeted for degradation (*rpoS*).

Figure 5.4 Expression of *E. coli* pMT41 (*csrB-luxCDABE*) promoter reporter. To reconstruct the UvrY-*csrB* pathway of *E. coli*, the promoter of *E. coli* K-12 *csrB* sRNA was cloned upstream of a promoterless *luxCDABE* cassette (pMT41). Regulation of the reporter was tested in *E. coli* MG1655 *uvrY33*::Tn5 mutant (*gacA* orthologous mutant) in the presence of *gacA* from *Serratia marcescens* PDL100 expressed from an arabinose-inducible promoter on pBAD18-*gacA*. The *gacA* plasmid was constructed as follows. Firstly, genomic *gacA* from *S. marcescens* PDL100 was amplified with Taq polymerase using primers ACATCTCAGGCTATAACAGAGGCTG and TCGTCACGCAAAAGAACATTATATC. The resulting ~1000 bp PCR fragment was gel purified and cloned into pCR2.1-TOPO PCR cloning vector, from which it was excised with EcoRI and subcloned into pBAD18, which was completely digested with EcoRI and treated with CIAP. The resulting construct was confirmed by sequencing. pBAD18-*gacA* carries resistance to ampicillin. Strains contained the

promoter reporter in the wild type *E. coli* MG1655 (), or *gacA* (*uvrY*) mutant RG133 (), with pBAD18-*gacA* in the presence of 50 mM arabinose () or with the pBAD18 vector control in the presence of arabinose (). The substitution of glucose for arabinose eliminated complementation by *gacA* borne on pBAD18-*gacA* ().

Figure 5.5 Typical results generated from an initial *lux* screen. *E. coli* MG1655 pMT41 serves as a positive control. *E. coli* MG1655 pTIM2442 is a control for non-csrB specific luminescence. *E. coli* RG133 pMT41, LB media only and blank wells all serve as negative controls. The graph shows luminescence activity of nine compounds which were selected for additional study from the 1280 compound Library of Pharmaceutically Active Compounds (LOPAC). Compounds with no inhibition or less than 1 log(CPS) counts were not considered. Most show an intermediate level of luminescence with similar counts between the pMT41 and pTIM2442 reporters indicating nonspecific inhibition. Only sanguinarine shows a significant csrB specific inhibition although log(CPS) counts are well below the *E. coli* RG133 pMT41 negative control.

Figure 5.6 Typical Results generated from a dilution series time course *lux* screen. *E. coli* MG1655 pMT41 serves as a positive control. *E. coli* MG1655 pTIM2442 is a control for non-csrB specific luminescence. *E. coli* RG133 pMT41 serves as the negative control. Eight threefold dilutions were used, 150–0.07 µM. (a) Results of the 3′-Azido-3′-deoxythymidine dilutions series, which represents strong nonspecific *lux* inhibition; these compounds are likely to inhibit bacterial growth. (b) Results of the stavudine dilution series, which represents high

tightened. (C) and (D) show how the deployment ropes should be tied with a weighted bridle to minimize excessive swinging in currents and waves. The buoys (D) maintain the rack at a constant depth in a tidal regime. (E) shows a rack attached to a T-boom for deeper water deployment. (Not to scale.)

Figure 6.2 (a) Example data presentation that is not correct as the bars are means across all levels of replication, in this case that includes field of view, replicate and block. The error bars are standard deviations. (b) This is also incorrect as the bars are means of all levels of replication and the use of 95% confidence intervals is therefore misleading and encourages the reader to eyeball the data and make subjective and, therefore, erroneous interpretations. This is the most common form of data display. (c) Probably the best way to present these data as the bars represent the estimated means from the generalized linear model and the errors indicated are simply standard deviations. (d) Treatment group centroids of two discriminant functions summarize all variables measured, including species data, for this experiment. There is a clear grouping of some treatments with the rest scattered across the plot. Interpretation requires examination of the two function matrices.

Figure 6.3 Ballast Organic Biofilm [BOB] sampler used to acquire biofilm samples in ballast water tanks.

Figure 6.4 Photo of tray of test plates (left). As shown on the right, two of these trays fit into the BOB sampler.

Figure 6.5 Amount of chlorophyll (μg cm^{-2}) on the rock surface in a single plot across sampling times: